Environmental Science & Technology

Article

pubs.acs.org/est

Molecular Characterization of Organosulfates in Organic Aerosols from Shanghai and Los Angeles Urban Areas by Nanospray-Desorption Electrospray Ionization High-Resolution Mass Spectrometry

Shikang Tao,[†,∥] Xiaohui Lu,[†,∥] Nicole Levac,[‡] Adam P. Bateman,[‡] Tran B. Nguyen,[‡] David L. Bones,[‡] Sergey A. Nizkorodov,[‡] Julia Laskin,[§] Alexander Laskin,*[,⊥] and Xin Yang*[,†,¶]

[†]Shanghai Key Laboratory of Atmospheric Particle Pollution and Prevention, Department of Environmental Science and Engineering, Fudan University, Shanghai 200433, China

[‡]Department of Chemistry, University of California, Irvine, California 92697, United States

[§]Physical Sciences Division and [⊥]William R. Wiley Environmental Molecular Sciences Laboratory, Pacific Northwest National Laboratory, Richland, Washington 99354, United States

[¶]Fudan Tyndall Centre, Fudan University, Shanghai 200433, China

Supporting Information

ABSTRACT: Fine aerosol particles in the urban areas of Shanghai and Los Angeles were collected on days that were characterized by their stagnant air and high organic aerosol concentrations. They were analyzed by nanospray-desorption electrospray ionization mass spectrometry with high mass resolution ($m/\Delta m$ = 100,000). Solvent mixtures of acetonitrile and water and acetonitrile and toluene were used to extract and ionize polar and nonpolar compounds, respectively. A diverse mixture of oxygenated hydrocarbons, organosulfates, organonitrates, and organics with reduced nitrogen were detected in the Los Angeles sample. A majority of the organics in the Shanghai sample were detected as organosulfates. The dominant organosulfates that were detected at two locations have distinctly different molecular characteristics. Specifically, the organosulfates in the Los Angeles sample were dominated by biogenic products, while the organosulfates of a yet unknown origin found in the Shanghai sample had distinctive characteristics of long aliphatic carbon chains and low degrees of oxidation and unsaturation. The use of the acetonitrile and toluene solvent facilitated the observation of this type of organosulfates, which suggests that they could have been missed in previous studies that relied on sample extraction using common polar solvents. The high molecular weight and low degree of unsaturation and oxidization of the uncommon organosulfates suggest that they may act as surfactants and plausibly affect the surface tension and hygroscopicity of atmospheric particles. We propose that direct esterification of carbonyl or hydroxyl compounds by sulfates or sulfuric acid in the liquid phase could be the formation pathway of these special organosulfates. Long-chain alkanes from vehicle emissions might be their precursors.

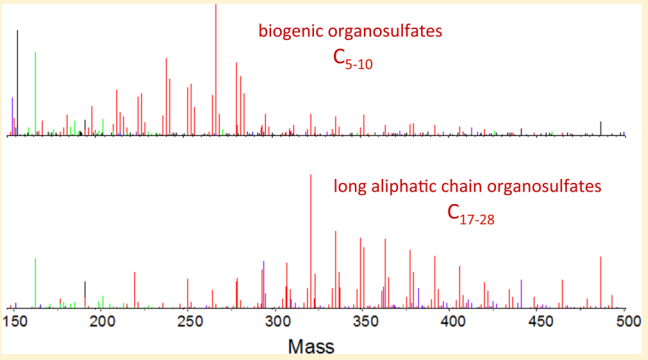

INTRODUCTION

Submicron atmospheric aerosols play an important role in climate change, air quality, and human health issues.[1−4] Organic compounds are important constituents of atmospheric aerosol particles.[5,6] Primary organic aerosols are emitted directly from sources such as fossil fuel combustion and biomass burning. Secondary organic aerosols (SOAs) are dominated by condensable products of the atmospheric oxidation of volatile organic compounds (VOCs) in the presence of O_3, OH radicals, NO_3 radicals, and other oxidants.[7] Organic aerosols contain partly oxidized hydrocarbons, organonitrates, amines or imines, organosulfates, and other compounds with a variety of oxygenated functional groups. Because of their significant contribution to the SOA yield, formation mechanisms and molecular-level characterization of organosulfates (esters of sulfuric acid, $ROS(O)_2OH$) have been the focus of many laboratory and field studies. Organosulfates are formed under highly acidic conditions by the reaction of sulfuric acid with SOA compounds containing a hydroxyl group.[8,9] They can also be formed under less acidic conditions by nucleophilic substitution reactions of sulfate with epoxides[10] and by free

Received: May 22, 2014
Revised: August 20, 2014
Accepted: August 21, 2014
Published: August 21, 2014

dx.doi.org/10.1021/es5024674 | Environ. Sci. Technol. 2014, 48, 10993−11001

radical mechanisms.[11] Because of their amphiphilicity, organosulfates may significantly affect the hygroscopic properties of aerosols.[12] High molecular weight (high-MW) organosulfates are also important constituents to humic-like substances (HULIS) in ambient aerosol,[13−15] and they are different from the terrestrial humic and fulvic acids.[16]

Smog chamber experiments by Surratt et al. showed that organosulfates contribute to enhanced SOA yields when the aerosol acidity increases, for example, as a result of anthropogenic SO_2 emissions.[17] Hence organosulfates are useful indicators of the unique chemistry between biogenic and anthropogenic emissions and resulting amplification of SOA formation. Since isoprene and monoterpenes (e.g., α- and β-pinene) are the major precursors of SOAs on a global scale, a number of organosulfates that are derived from these biogenic VOCs have been identified in lab and field studies.[8,9,18−21]

The contribution of organosulfates derived from biogenic VOCs to organic aerosols exhibits a seasonal variation. For example, Ma et al.[22] showed that organosulfates derived from biogenic VOCs in Shanghai were more prevalent in the summer than in the other seasons. The seasonal trends can be different in different regions. For example, seasonal cycles of organosulfates derived from biogenic VOCs in tropical and subtropical regions of Asia[23] are not as pronounced as those in the midwestern United States.[24] On the other hand, organosulfates derived from anthropogenic VOCs have gained attention because they are suggested as potential tracers for SOA formation from anthropogenic VOCs, for example, organosulfates with aromatic characteristics that were detected in Lahore, Pakistan potentially originate from industry-generated precursors.[25] Since organosulfates in urban areas are strongly related to anthropogenic emissions and human activities, aerosols in different cities could contain different types of organosulfates. However, the molecular-level composition of organosulfates, especially the high-MW organosulfates, between different metropolises at the time of elevated air pollution has not been systematically compared.

This work compares the organic compounds, especially organosulfates, in the aerosol samples collected in two coastal metropolises, Shanghai (SH) and Los Angeles (LA) during a typical day in spring characterized by high concentrations of organic aerosols. We observed and characterized a new class of organosulfates, which might be specific to anthropogenic emissions and secondary chemistry in selected urban environments. We use nanospray desorption electrospray ionization high-resolution mass spectrometry (nano-DESI HR-MS)[26] for the detailed molecular-level characterization of the particulate matter samples. Nano-DESI offers considerable advantages over traditional electrospray ionization (ESI) including low sample requirements, in situ extraction, and short solvent−analyte interaction time.[27−30] Another advantage that is critical to this work is its ability to analyze the same sample using different extraction solvents.[31] In this study, we used both acetonitrile/water (AcN/H_2O) and acetonitrile/toluene (AcN/Tol) mixtures to probe a wider range of compounds in the aerosol samples. The use of AcN/Tol enables the characterization of less polar organosulfates that are difficult to observe using more traditional polar solvents for sample extraction.

EXPERIMENTAL SECTION

At an urban site in Pasadena, Los Angeles, aerosols with aerodynamic sizes of 0.32−0.56 μm were collected as the LA sample from noon−6 p.m. (local time) on May 19, 2010 when real-time records of an aerosol mass spectrometer (AMS)[32] showed the highest organic aerosol concentration in ambient air during the CalNex field study (May 15−June 14, 2010).[33] Similarly, at Fudan University, Shanghai, aerosols with aerodynamic sizes of 0.4−0.7 μm were collected as the SH sample from 6 a.m.−6 p.m. (local time) on April 15, 2011 when the carbonaceous compounds in the atmospheric aerosols had the highest concentration during the April 10−April 20, 2011 period (Figure S1, Supporting Information). The hybrid single particle Lagrangian integrated trajectory (HYSPLIT) model was used to calculate the backward trajectories of the air masses that arrived at the sampling sites (Figure S2, Supporting Information) and showed that the particulates in both cases corresponded to the low-wind continental air masses that stayed within the urban surface boundary layer for 6−12 h prior to the sampling. Both the LA sample and the SH sample were analyzed by nano-DESI HR-MS for in-depth molecular characterization. A more detailed description of the sampling, selection of the characteristic samples for in-depth analysis, application of nano-DESI HR-MS platform for molecular characterization, peak assignments, and associated data analysis tools are included in the Supporting Information.

RESULTS

Mass Spectra and Elemental Composition. Each sample has four different sets of MS data that were acquired in positive and negative modes using AcN/H_2O or AcN/Tol solvents. Throughout the manuscript, we will refer to the different spectra using an abbreviated notation that includes the city code, solvent, and ion mode. For example, SH AcN/H_2O(+) MS indicates a positive mode mass spectrum of the aerosol sample from Shanghai, extracted and ionized using the AcN/H_2O solvent. The mass spectra are shown in Figure 1 (negative ion mode) and Figure S3 of the Supporting Information (positive ion mode). The peak numbers and number fractions of various species after formula assignments are summarized in Table 1. The compounds assigned as $C_cH_hO_oN_nS_s$ with $n = 0$ and $s = 0$ will be referred to as CHO; those with only $s = 0$ will be referred to as CHON; those with $n = 0$ and $s = 1,2$ will be referred to as CHOS; those with $s = 0$, $o = 0$ and $n > 0$ will be referred to as CHN; and those that contain all five elements will be referred to as CHONS. The nitrogen-containing organic compounds (CHN, CHON, and CHONS) will be collectively referred to as N−OC, while the sulfur-containing organic compounds (CHOS and CHONS) will be referred to as S−OC.

Difference between AcN/H_2O and AcN/Tol MS. Table 1 demonstrates that more MS peaks were observed when the AcN/Tol solvent was used than when the AcN/H_2O solvent was used. To illustrate the differences in the mass spectra, we summarized the peak numbers in the different mass ranges in Figure 2 and Figure S4 of the Supporting Information. The peak number distribution is shifted toward the high-MW compounds in AcN/Tol MS, which is consistent with the observation in Eckert's work.[31] This effect is especially apparent for S−OC species observed in the negative mode and N−OC species observed in the positive mode, which suggests that AcN/Tol enables a better extraction of high-MW species than does AcN/H_2O.

The organic aerosol compounds observed in AcN/H_2O and AcN/Tol MS likely have different polarities. This suggestion can be inferred from the assigned molecular formulas as illustrated by the van Krevelen[34] diagrams of Figure 3, which

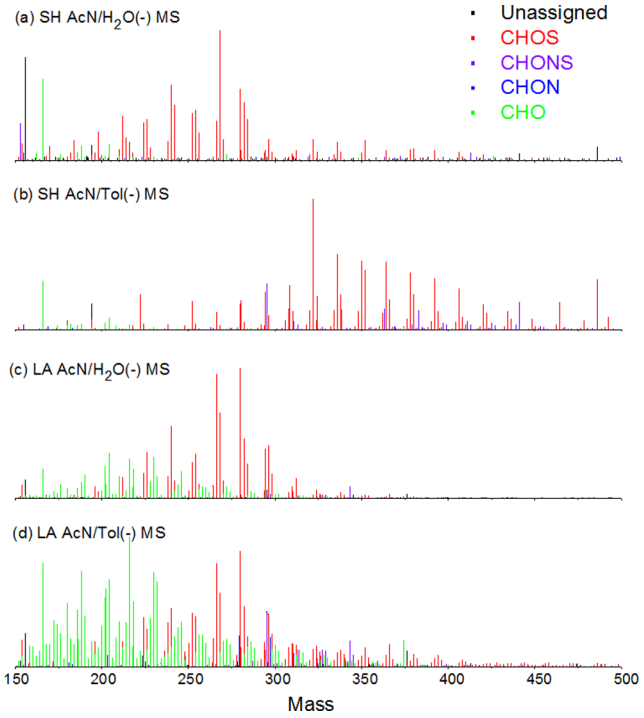

Figure 1. Nano-DESI HR-MS reconstructed mass spectra in the negative ion mode. *X*-axis corresponds to the molecular weight of the neutral species (Da). Different formula groups are color-coded. The unassigned peaks were converted into "neutral mass" on the assumption that they were deprotonated.

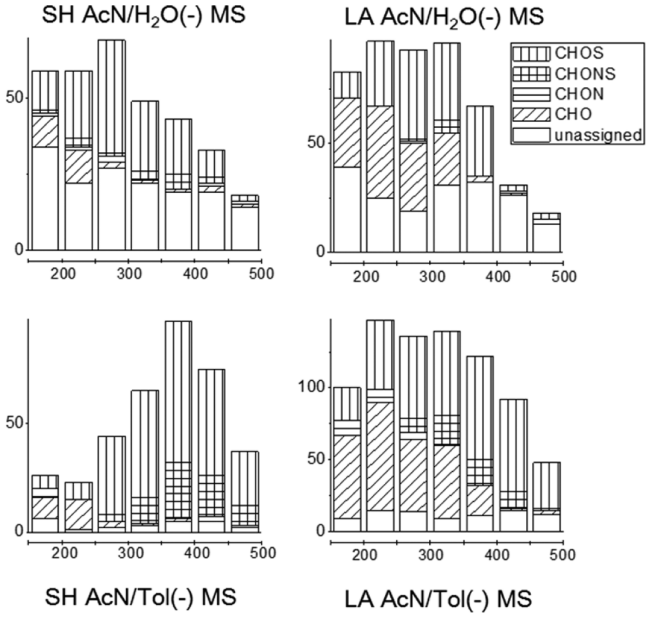

Figure 2. Number fraction of different species in the different mass ranges (negative mode). The bins are 50 Da wide.

indicate that the characteristic species observed in AcN/Tol MS have a lower O/C ratio than do those observed in AcN/H_2O MS, especially for the LA sample. Since the higher O/C ratio is associated with the polar functional groups, the data of Figure 3 demonstrates that less polar (less oxygenated) organic compounds in aerosols are better desorbed and ionized by the use of AcN/Tol as the working solvent.

Difference between the SH and LA Samples. For the LA sample, most of the peaks were unambiguously assigned with molecular formulas. CHO and N−OC compounds dominated in the positive mode, while in the negative mode, CHO and S−OC were more abundant. But for the SH sample, approximately half of the peaks could not be unambiguously assigned within the applied constrains of the formula search. S−OC in the negative mode accounted for the majority (nearly 80%) of all of the assigned compounds. One plausible reason for the poor observation of CHO and CHON is that the heavily loaded inorganic species in the SH sample may have caused ionization suppression. Another reason is that the heavy pollution in Shanghai leads to a very high concentration of sulfuric acid, which facilitates the conversion of the organic compounds into organosulfates. Alkyl nitrates (members of the CHON group) may be too volatile and require additional functionalization to CHONS before they can efficiently partition to the particle phase.[10,35] Indeed, the organonitrates observed in the SH sample (and also in the LA sample) were mostly assigned to the CHONS species. Finally, compared to the organosulfates, the organonitrates are less stable with respect to nucleophilic substitution reactions with water or sulfate.[10,36] A more detailed analysis of CHO and N−OC species is included in the Supporting Information.

Analysis of S−OC Compounds. S−OC species were very abundant in the negative ion mode for both locations. High-MW S−OC was more readily observed using the AcN/Tol rather than the AcN/H_2O solvent, which is likely a result of differences in the analyte solubility in these two solvents. Considering the lower polarity of AcN/Tol relative to that of AcN/H_2O, the high-MW S−OC species appear to be less polar and less water-soluble than the low-MW S−OC species.

More than 93% of S−OC species in both samples contained one S atom and more than four O atoms ($s = 1$ and $o > 7$ for CHONS) and were observed only in the negative mode. These S−OC compounds with one S atom are abbreviated as $CHOS_1$ and $CHONS_1$ in this manuscript. The fractions of $CHOS_1$ and

Table 1. Summary of Peaks Observed in Nano-DESI HR-MS. Values in Parentheses are the Percent Fractions of Different Species among the Assigned Peaks

MS	unassigned	CHO	CHN	CHON	CHONS	CHOS
SH AcN/H_2O (+) MS	39	20 (67%)	0	2 (7%)	0	8 (27%)
SH AcN/H_2O (−) MS	157	28 (16%)	0	6 (3%)	15 (9%)	124 (72%)
SH AcN/Tol (+) MS	92	15 (41%)	0	15 (41%)	1 (3%)	6 (16%)
SH AcN/Tol (−) MS	24	29 (8%)	0	7 (2%)	69 (20%)	238 (69%)
LA AcN/H_2O (+) MS	40	177 (50%)	1 (0%)	174 (49%)	1 (0%)	2 (1%)
LA AcN/H_2O (−) MS	185	134 (45%)	0	4 (1%)	7 (2%)	156 (52%)
LA AcN/Tol (+) MS	57	221 (32%)	10 (1%)	448 (66%)	1 (0%)	3 (0%)
LA AcN/Tol (−) MS	85	259 (37%)	0	25 (4%)	60 (9%)	355 (51%)

dx.doi.org/10.1021/es5024674 | *Environ. Sci. Technol.* 2014, 48, 10993−11001

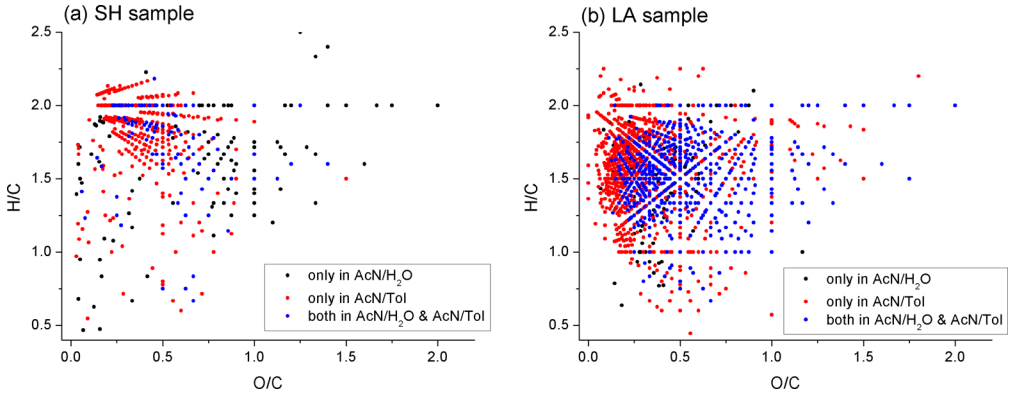

Figure 3. Van Krevelen diagrams for the assigned organic aerosols observed in the (a) SH sample and (b) LA sample. Color-coding indicates the compounds observed only in AcN/H_2O MS (black), only in AcN/Tol MS (red), and in both AcN/H_2O and AcN/Tol MS (blue).

Table 2. Summary of CHOS and CHONS Species Observed in Negative Mode. Subgroup B Refers to Aliphatic Organosulfates with Little or No Substitution by Other Functional Groups

MS	CHOS	$CHOS_1$	subgroup B CHOS	CHONS	$CHONS_1$	subgroup B CHONS
SH AcN/H_2O (−) MS	124	120	40	15	5	2
SH AcN/Tol (−) MS	238	236	112	69	69	40
LA AcN/H_2O (−) MS	156	156	13	7	7	1
LA AcN/Tol (−) MS	355	327	59	60	58	6

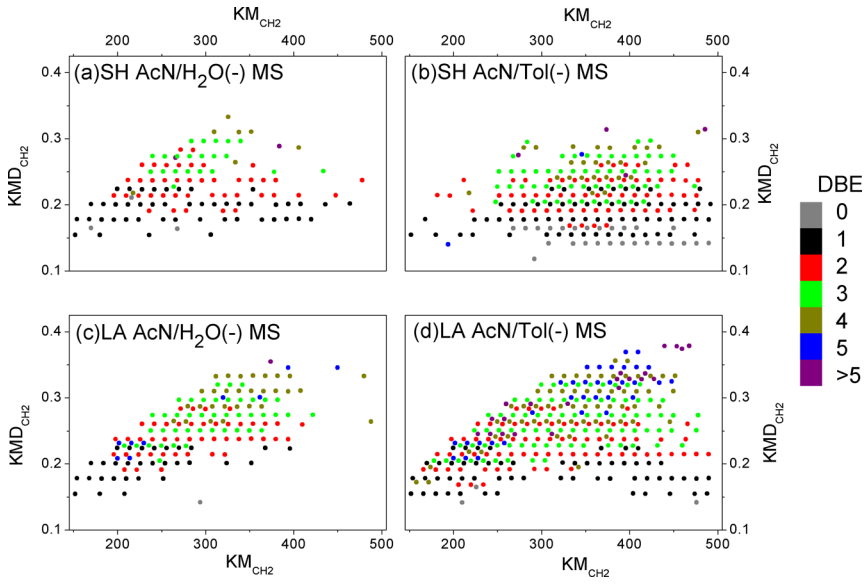

Figure 4. CH_2 Kendrick diagrams for the $CHOS_1$ detected in (a) SH AcN/H_2O(−) MS, (b) SH AcN/Tol(−) MS, (c) LA AcN/H_2O(−) MS, and (d) LA AcN/Tol(−) MS. The color-coding indicates the DBE values calculated from eq S1 of the Supporting Information.

$CHONS_1$ peaks are listed in Table 2. Since a sulfate group ($-OSO_3H$) carries four oxygen atoms and it readily deprotonates in ESI, $CHOS_1$ and $CHONS_1$ are likely organosulfates. Since $CHOS_1$ and $CHONS_1$ contribute to both the most apparent similarity and the most apparent difference between the SH and LA samples, we carried out a detailed analysis and compared them below.

$CHOS_1$. Figure 4 shows the CH_2 Kendrick diagrams of the observed $CHOS_1$ species. The variation in the double bond equivalent (DBE) values is shown by the color mapping. The majority of the observed compounds have DBE values below 5. (Since the DBE value is calculated from eq S1, as discussed in the Supporting Information, the value is 2 units lower than the true value for organosulfates.) For either the SH or LA sample, the average size of the CH_2 families that were observed in the Kendrick diagram of AcN/Tol(−) MS is larger than that in AcN/H_2O(−) MS diagram, which suggests that long-chain CHOS compounds are better extracted in a less polar AcN/Tol solvent. The average family size is larger in the SH sample than in the LA sample. A comparison of Figure 4 with the CH_2O Kendrick diagram (Figure S8, Supporting Information) suggests that CH_2 is not the unique Kendrick base for the LA sample. The average size of the CH_2O families is larger in the LA sample than in the SH sample. These observations indicate that the $CHOS_1$ species in the SH sample are more aliphatic than those detected in the LA sample.

To illustrate the occurrences of $CHOS_1$ species with various numbers of O atoms and various DBE values, we reconstructed

dx.doi.org/10.1021/es5024674 | Environ. Sci. Technol. 2014, 48, 10993−11001

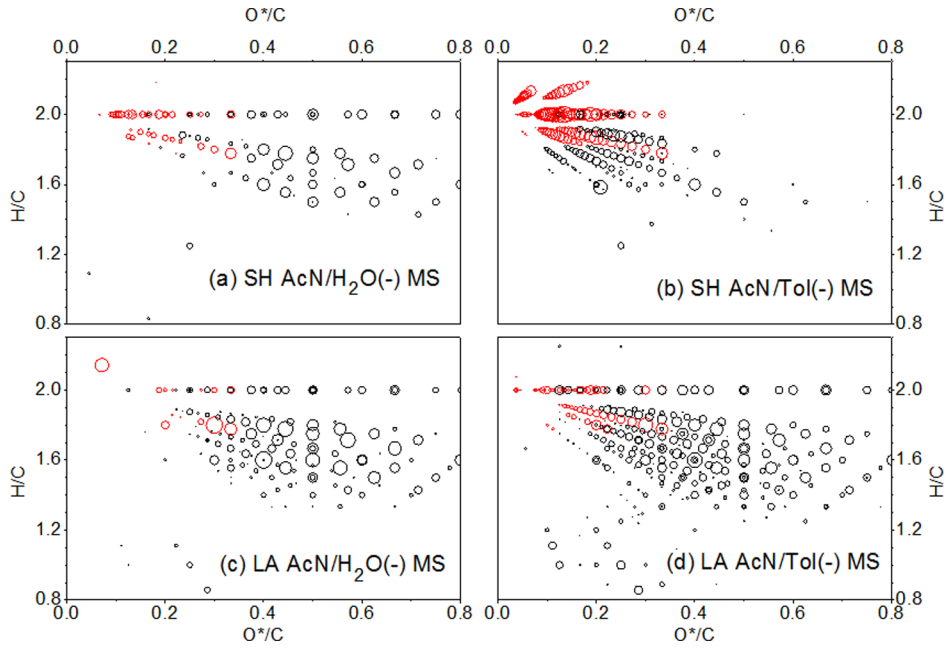

Figure 5. Van Krevelen diagrams constructed by plotting the H/C ratio against the O*/C = (O − 3)/C ratio for $CHOS_1$ species detected in (a) SH AcN/H_2O(−) MS, (b) SH AcN/Tol(−) MS, (c) LA AcN/H_2O(−) MS, and (d) LA AcN/Tol(−) MS. The size of the circles is proportional to the logarithm of the corresponding peak intensity. Cycles of the subgroup B (aliphatic organosulfates species) are red.

the mass spectra of $CHOS_1$ by color-coding the peaks by DBE value (Figure S9) or by the number of O atoms (Figure S10). Several CH_2 homologous series of $CHOS_1$ compounds that share an identical DBE and O number are clearly observed in the spectra. The main difference between $CHOS_1$ in the SH and LA samples is the higher abundance of $CHOS_1$ with DBE values < 3 and O numbers < 7 in the SH sample. The strongest peaks in SH AcN/Tol(−) MS correspond to a lower DBE, fewer O atoms, and a higher molecular weight than those in the other three spectra. The $(CH_2)_nO_5S$ series (the overlap of black-colored peaks in Figure S9 and red-colored peaks in Figure S10) is the most abundant family among these high-MW compounds. These species are most likely organosulfates, R−OSO_3H, with an additional carbonyl group in the aliphatic chain R; however, they could also be organosulfates with a hydroxyl group and a C═C bond or cycle in the side chain.

Figure 5 shows a Van Krevelen (VK) plot that additionally illustrates the differences between the $CHOS_1$ species detected in the two samples. Because the formation of organosulfates involves either the esterification of an −OH group (net addition of SO_3 to the reactant) or the opening of epoxides (net addition of H_2SO_4 to the reactant),[8,10,11] we constructed the VK diagram by plotting the H/C ratio versus the modified O*/C ratio (where O* = O − 3). Since the sulfate group contains three more oxygen atoms than do common oxygen-containing groups such as hydroxyl and carbonyl, the use of O*/C instead of O/C better illustrates the number of additional oxidized groups per carbon atom. In the VK diagram of SH AcN/Tol(−), the majority of points have a high H/C ratio (>1.6) and a low O*/C ratio (<0.3), which indicates a low degree of oxidation and unsaturation. Points with the same DBE value form a series of lines that intersect at the crossover position of H/C = 2 and O*/C = 0. These series of lines correspond to the long horizontal lines in the CH_2 Kendrick diagram (Figure 4). The dense distribution of points within the region near the crossover position reflects the presence of long alkyl-chains in many $CHOS_1$ species of the SH sample. In contrast, the characteristic data points of the LA sample are mainly distributed in the region of the VK plot with 0.3 < O*/C < 0.8. Though some points were observed in the top−left part of the VK diagram of LA AcN/Tol(−), their distribution is less dense than that of the SH sample. These observations are consistent with higher degree of saturation and lower degree of oxidation of the $CHOS_1$ species in the SH sample compared to those in the LA sample.

$CHONS_1$. $CHONS_1$ species are minor in both the SH and LA samples. The CH_2 Kendrick and VK diagrams of $CHONS_1$ (Figure S11, Supporting Information) look qualitatively similar to the corresponding diagrams of $CHOS_1$. Once again, $CHONS_1$ species in the SH sample have substantially longer carbon chain lengths than do those in the LA sample. The $CHONS_1$ species in the SH sample have higher H/C ratios (with a number of compounds with H/C ≈ 2) and lower DBE values than do those in the LA sample. The KMD_{CH2} values of $CHONS_1$ are generally larger than those of $CHOS_1$, but this can be explained by the contribution of N atoms to KMD_{CH2}. The higher O*/C ratio for $CHONS_1$ than for $CHOS_1$ in the VK diagrams as well as the higher O/N ratio (Figure S6, Supporting Information) suggest that the observed $CHONS_1$ species might be nitrooxy organosulfates.[8]

■ DISCUSSION AND ATMOSPHERIC IMPLICATIONS

Subgroups of Organosulfates. On the basis of the observed differences of S−OC between the SH and LA samples, we can divide the detected organosulfates into two classes. Subgroup A includes the organosulfates that can be attributed to common SOA precursors and their derivatives. Subgroup B includes uncommon organosulfates with characteristic long alkyl carbon chains, containing a few or no additional functional groups. For the purposes of this study, we define subgroup B (red points in VK diagrams in Figure 5 and Figure S11, Supporting Information) as $CHOS_1$ with C > 8, DBE < 3, and 3 < O < 7 and $CHONS_1$ with C > 8, DBE < 3, and 6 < O <

10. High-MW and low degrees of unsaturation and oxidation are the characteristic features of subgroup B.

Subgroup B compounds represent the main difference between S−OC species in the SH and LA samples, which is summarized in Table 2. Out of all of the S−OC species observed in SH AcN/Tol(−) MS, subgroup B species account for nearly 50% (by number), while they are less than 16% in LA AcN/Tol(−) MS. Species of subgroup B occur as continuous homologous CH_2 series, which indicates their chemical homogeneity. For example, out of 112 species of the CHOS subgroup B in SH AcN/Tol(−) MS, only seven compounds were not a part of any continuous CH_2 series. The $(CH_2)_nO_5S$ series was observed as the most abundant and characteristic subset of subgroup B. As discussed above, these series can be constructed by functionalizing a saturated hydrocarbon with one sulfate and one carbonyl group. In addition, we observed compounds that were even less oxidized such as $(CH_2)_nH_2O_4S$, which corresponds to saturated hydrocarbons that were functionalized with only one sulfate group. Another feature of subgroup B is the low polarity due to the long alkyl-chain, which enables them to be better dissolved and ionized in a less polar solvent such as AcN/Tol.

Possible Origin of Subgroup B Organosulfates. The most abundant CHOS peaks in all negative spectra are listed in Table S1 of the Supporting Information and compared with the characteristic masses of organosulfates reported in laboratory studies of biogenic VOC oxidation.[8,9] With the exception of SH AcN/Tol(−) MS, most of the peaks with a relative intensity higher than 30% in all other spectra are consistent with the biogenic VOC-derived organosulfates, and they primarily belong to subgroup A organosulfates. Therefore, subgroup A can be plausibly organosulfates of a biogenic origin that have been affirmed in previous laboratory studies.[8,9] Several organosulfates ($C_5H_{10}O_6S$, $C_5H_{10}O_5S$, and $C_5H_8O_6S$) potentially traceable to isoprene (C_5H_8) were observed in both the SH and LA samples; however, 2-methyltetrol sulfated esters ($C_5H_{12}O_7S$), the most abundant isoprene-related organosulfates reported so far in several studies,[8,37] were not detected. This indicates that the observed C5 organosulfates might be formed from other precursors. The fact that C6, C7, and C8 organosulfates are more abundant than the C5 species (Table S1, Supporting Information) suggests that isoprene is a relatively minor contributor to the population of organosulfates in the LA and SH samples we examined.

In contrast, species of subgroup B contribute to the majority of peaks with a relative intensity higher than 30% in SH AcN/Tol(−) MS, but their characteristic formulas are different from the reported isoprene- and terpene-derived organosulfates. The formation of organosulfates from terpenes involves the oxidation by ozone, nitrate radical, or hydroxyl radical that leads to their oxygenated products that typically contain more than one functional group (and often partially retain the skeleton of the precursor terpene). The oxidized compounds subsequently react with the particulate sulfates or sulfuric acid to form organosulfates.[8] As a result, organosulfates derived from terpenes are expected to have high degree of oxidation and DBE values close to those of their terpene precursors. However, subgroup B CHOS species have fewer than three O atoms in addition to the four O atoms that belong to the sulfate group. The low oxygen content and low DBE value (< 3) make them inconsistent with the biogenic origin of their precursors.

Recent laboratory work by Nguyen et al.[38] reported that the evaporation of aqueous extracts of limonene-derived SOAs with sulfuric acid (pH = 2) results in the production of high-MW organosulfates through a ring-opening reaction of epoxides or through the direct esterification of alcohols or enols. The $(CH_2)_nH_2O_4S$ (n = 17−28) compounds, which form a prominent family within subgroup B (the gray points with KMD_{CH2} of ca. 0.142 in Figure 4b), can only be produced by the direct esterification of an aliphatic alcohol. Compounds with a larger number of oxygen atoms or higher DBE values could be produced by either ring-opening or an epoxide mechanism. We note that the SH sample was collected diurnally and particles in urban areas of Chinese metropolises are highly acidic.[39−41] Daytime warming leads to the evaporation of water from the aerosol particles and possible enhancement of the esterification of hydroxyl/enol compounds with sulfuric acid. Regardless of the mechanism, the low degree of oxidation of group B organosulfates suggests that their precursors are long alkyl-chain compounds with few oxygenated functional groups. The subgroup B species could not be products of typical oligomerization processes, which proceeds through aldol condensation. In that case, they should have contained more O atoms and double bonds.[42,43]

We propose that the possible precursors for subgroup B organosulfates are long-chain alkanes from traffic emissions. Studies on diesel engine nanoparticles have shown that alkanes and cycloalkanes from unburned fuel and lubricating oil contribute to the majority of the diesel particle mass and their alkane carbon numbers are generally more than 10.[44,45] On the basis of measurements by Schauer et al.,[46,47] long-chain alkanes are major components of tailpipe emissions from medium duty diesel trucks and gasoline powered motor vehicles. Long-chain alkanes are decorated with carbonyl and hydroxyl groups on a time scale of hours under typical urban conditions.[48,49] Afterward, the long-chain carbonyl or hydroxyl compounds can be esterified to form subgroup B organosulfates. Given the heavy traffic but poorly maintained motors in Chinese metropolises, a large amount of subgroup B organosulfates emerge, facilitated by the stagnating air mass and high degree of atmospheric acidity of Shanghai. In addition to the roadway vehicle emissions, petrochemical industry,[50,51] incomplete biomass burning,[52] and cooking[53,54] are also possible emission sources for long-chain hydrocarbons as the precursors of subgroup B organosulfates. Over the past decade, aromatic VOCs have been widely studied as an important source of particulate air-pollution in populated areas like urban Shanghai.[55,56] Our results suggest that the long-chain hydrocarbons, and the organosulfates produced from them, also play an important role in the formation of particulate matter.

Atmospheric Implications of Subgroup B Organosulfates. The hydrophilic (sulfate group) and hydrophobic (long alkyl chains) functionalities suggest that subgroup B compounds have surfactant properties and therefore may have a significant impact on the properties of particles. Surfactant sulfur-containing aerosols that originate from proteins, lipids, and oligosaccharide complexes in marine biota previously have been observed in the marine boundary layer.[57] Linear alkylbenzenesulfonates were also reported in atmospheric coastal aerosols;[58] however, the organosulfates of subgroup B are significantly different from the previously reported S-containing surfactants because they exhibit a lower degree of unsaturation and oxidation, and have long CH_2 homologous series. Subgroup B organosulfates are likely to form more ordered surfactant films on the aerosols, which would decrease the surface tension and plausibly affect the hygroscopicity of

particles.[59] The $(CH_2)_nO_5S$ series of subgroup B organosulfates was also observed by Lin et al.[15] in the urban area of Guangzhou (a megacity in South China). On the basis of this limited number of observations, subgroup B organosulfates might be characteristic of aerosols in large Chinese cities, possibly because of the dense population and heavy traffic there. However, these types of compounds may be more common, and one possible reason for the paucity of prior observations of these organosulfates is that the long alkyl-chain and few polar groups make them less soluble in polar solvents traditionally used for ESI-MS analysis such as AcN/H_2O and $MeOH/H_2O$. Our work shows that less polar AcN/Tol solvent is a better choice for the detection of this type of organosulfates.

■ ASSOCIATED CONTENT

Supporting Information

Additional information as noted in text. This material is available free of charge via the Internet at http://pubs.acs.org.

■ AUTHOR INFORMATION

Corresponding Authors

*Phone: 509-371-6129; fax: 509-371-6139; e-mail: alexander.laskin@pnl.gov.

*Phone: 86-21-55665272; fax: 86-21-55662020; e-mail: yangxin@fudan.edu.cn.

Author Contributions

‖S.T. and X.L. contributed equally to the work.

Notes

The authors declare no competing financial interest.

■ ACKNOWLEDGMENTS

The Fudan group acknowledges support by the National Natural Science Foundation of China (21177027, 41275126), the Ministry of Science and Technology of China (2012YQ220113-4), the Science and Technology Commission of Shanghai Municipality (12DJ1400100, 14XD1400600), and the Jiangsu Provincial Collaborative Innovation Center of Climate Change. X.L. acknowledges support from the Scholarship Award for Excellent Doctoral Student granted by the Ministry of Education of the P.R. China. N.L., A.P.B., T.B.N., D.L.B., S.A.N., J.L., and A.L. acknowledge the support from the U.S. Department of Commerce, National Oceanic and Atmospheric Administration through the Climate Program Office's AC4 program, and awards NA13OAR4310066 (PNNL) and NA13OAR4310062 (UCI). The nano-DESI/HR-MS experiments described in this paper were performed at the Environmental molecular Sciences Laboratory, a national scientific user facility that is sponsored by the U.S. DOE's Office of Biological and Environmental Research and is located at the Pacific Northwest National Laboratory (PNNL). PNNL is operated for the U.S. DOE by Battelle Memorial Institute under Contract No. DE-AC06-76RL0 1830.

■ REFERENCES

(1) Ramanathan, V.; Crutzen, P. J.; Kiehl, J. T.; Rosenfeld, D. Atmosphere, aerosols, climate, and the hydrological cycle. *Science* **2001**, *294* (5549), 2119−2124.

(2) Poschl, U. Atmospheric aerosols: Composition, transformation, climate, and health effects. *Angew. Chem., Int. Ed.* **2005**, *44* (46), 7520−7540.

(3) Kanakidou, M.; Seinfeld, J. H.; Pandis, S. N.; Barnes, I.; Dentener, F. J.; Facchini, M. C.; Van Dingenen, R.; Ervens, B.; Nenes, A.; Nielsen, C. J.; Swietlicki, E.; Putaud, J. P.; Balkanski, Y.; Fuzzi, S.; Horth, J.; Moortgat, G. K.; Winterhalter, R.; Myhre, C.; Tsigaridis, K.; Vignati, E.; Stephanou, E. G.; Wilson, J. Organic aerosol and global climate modelling: A review. *Atmos. Chem. Phys.* **2005**, *5*, 1053−1123.

(4) Menon, S.; Unger, N.; Koch, D.; Francis, J.; Garrett, T.; Sednev, I.; Shindell, D.; Streets, D. Aerosol climate effects and air quality impacts from 1980 to 2030. *Environ. Res. Lett.* **2008**, *3*, DOI: 10.1088/1748-9326/3/2/024004.

(5) Jacobson, M. C.; Hansson, H. C.; Noone, K. J.; Charlson, R. J. Organic atmospheric aerosols: Review and state of the science. *Rev. Geophys.* **2000**, *38* (2), 267−294.

(6) Fuzzi, S.; Andreae, M. O.; Huebert, B. J.; Kulmala, M.; Bond, T. C.; Boy, M.; Doherty, S. J.; Guenther, A.; Kanakidou, M.; Kawamura, K.; Kerminen, V. M.; Lohmann, U.; Russell, L. M.; Poschl, U. Critical assessment of the current state of scientific knowledge, terminology, and research needs concerning the role of organic aerosols in the atmosphere, climate, and global change. *Atmos. Chem. Phys.* **2006**, *6*, 2017−2038.

(7) Hallquist, M.; Wenger, J. C.; Baltensperger, U.; Rudich, Y.; Simpson, D.; Claeys, M.; Dommen, J.; Donahue, N. M.; George, C.; Goldstein, A. H.; Hamilton, J. F.; Herrmann, H.; Hoffmann, T.; Iinuma, Y.; Jang, M.; Jenkin, M. E.; Jimenez, J. L.; Kiendler-Scharr, A.; Maenhaut, W.; McFiggans, G.; Mentel, T. F.; Monod, A.; Prevot, A.; Seinfeld, J. H.; Surratt, J. D.; Szmigielski, R.; Wildt, J. The formation, properties, and impact of secondary organic aerosol: Current and emerging issues. *Atmos. Chem. Phys.* **2009**, *9* (14), 5155−5236.

(8) Surratt, J. D.; Gomez-Gonzalez, Y.; Chan, A.; Vermeylen, R.; Shahgholi, M.; Kleindienst, T. E.; Edney, E. O.; Offenberg, J. H.; Lewandowski, M.; Jaoui, M.; Maenhaut, W.; Claeys, M.; Flagan, R. C.; Seinfeld, J. H. Organosulfate formation in biogenic secondary organic aerosol. *J. Phys. Chem. A* **2008**, *112* (36), 8345−8378.

(9) Chan, M. N.; Surratt, J. D.; Chan, A.; Schilling, K.; Offenberg, J. H.; Lewandowski, M.; Edney, E. O.; Kleindienst, T. E.; Jaoui, M.; Edgerton, E. S.; Tanner, R. L.; Shaw, S. L.; Zheng, M.; Knipping, E. M.; Seinfeld, J. H. Influence of aerosol acidity on the chemical composition of secondary organic aerosol from beta-caryophyllene. *Atmos. Chem. Phys.* **2011**, *11* (4), 1735−1751.

(10) Darer, A. I.; Cole-Filipiak, N. C.; O'Connor, A. E.; Elrod, M. J. Formation and stability of atmospherically relevant isoprene-derived organosulfates and organonitrates. *Environ. Sci. Technol.* **2011**, *45* (5), 1895−1902.

(11) Perri, M. J.; Lim, Y. B.; Seitzinger, S. P.; Turpin, B. J. Organosulfates from glycolaldehyde in aqueous aerosols and clouds: Laboratory studies. *Atmos. Environ.* **2010**, *44* (21−22), 2658−2664.

(12) Pang, Y.; Turpin, B. J.; Gundel, L. A. On the importance of organic oxygen for understanding organic aerosol particles. *Aerosol Sci. Technol.* **2006**, *40* (2), 128−133.

(13) Romero, F.; Oehme, M. Organosulfates—A new component of humic-like substances in atmospheric aerosols? *J. Atmos. Chem.* **2005**, *52* (3), 283−294.

(14) Lin, P.; Rincon, A. G.; Kalberer, M.; Yu, J. Z. Elemental composition of HULIS in the Pearl River Delta region, China: Results inferred from positive and negative electrospray high resolution mass spectrometric data. *Environ. Sci. Technol.* **2012**, *46* (14), 7454−7462.

(15) Lin, P.; Yu, J. Z.; Engling, G.; Kalberer, M. Organosulfates in humic-like substance fraction isolated from aerosols at seven locations in East Asia: A study by ultra-high-resolution mass spectrometry. *Environ. Sci. Technol.* **2012**, *46* (24), 13118−13127.

(16) Stone, E. A.; Hedman, C. J.; Sheesley, R. J.; Shafer, M. M.; Schauer, J. J. Investigating the chemical nature of humic-like substances (HULIS) in North American atmospheric aerosols by liquid chromatography tandem mass spectrometry. *Atmos. Environ.* **2009**, *43* (27), 4205−4213.

(17) Surratt, J. D.; Kroll, J. H.; Kleindienst, T. E.; Edney, E. O.; Claeys, M.; Sorooshian, A.; Ng, N. L.; Offenberg, J. H.; Lewandowski, M.; Jaoui, M.; Flagan, R. C.; Seinfeld, J. H. Evidence for organosulfates in secondary organic aerosol. *Environ. Sci. Technol.* **2007**, *41* (2), 517−527.

(18) Walser, M. L.; Desyaterik, Y.; Laskin, J.; Laskin, A.; Nizkorodov, S. A. High-resolution mass spectrometric analysis of secondary organic aerosol produced by ozonation of limonene. *Phys. Chem. Chem. Phys.* **2008**, *10* (7), 1009−1022.
(19) Carlton, A. G.; Wiedinmyer, C.; Kroll, J. H. A review of secondary organic aerosol (SOA) formation from isoprene. *Atmos. Chem. Phys.* **2009**, *9* (14), 4987−5005.
(20) Iinuma, Y.; Muller, C.; Berndt, T.; Boge, O.; Claeys, M.; Herrmann, H. Evidence for the existence of organosulfates from beta-pinene ozonolysis in ambient secondary organic aerosol. *Environ. Sci. Technol.* **2007**, *41* (19), 6678−6683.
(21) Zhang, H. F.; Worton, D. R.; Lewandowski, M.; Ortega, J.; Rubitschun, C. L.; Park, J. H.; Kristensen, K.; Campuzano-Jost, P.; Day, D. A.; Jimenez, J. L.; Jaoui, M.; Offenberg, J. H.; Kleindienst, T. E.; Gilman, J.; Kuster, W. C.; de Gouw, J.; Park, C.; Schade, G. W.; Frossard, A. A.; Russell, L.; Kaser, L.; Jud, W.; Hansel, A.; Cappellin, L.; Karl, T.; Glasius, M.; Guenther, A.; Goldstein, A. H.; Seinfeld, J. H.; Gold, A.; Kamens, R. M.; Surratt, J. D. Organosulfates as tracers for secondary organic aerosol (SOA) formation from 2-methyl-3-buten-2-ol (MBO) in the atmosphere. *Environ. Sci. Technol.* **2012**, *46* (17), 9437−9446.
(22) Ma, Y.; Xu, X.; Song, W.; Geng, F.; Wang, L. Seasonal and diurnal variations of particulate organosulfates in urban Shanghai, China. *Atmos. Environ.* **2014**, *85*, 152−160.
(23) Stone, E. A.; Yang, L. M.; Yu, L.; Rupakheti, M. Characterization of organosulfates in atmospheric aerosols at four Asian locations. *Atmos. Environ.* **2012**, *47*, 323−329.
(24) Lewandowski, M.; Jaoui, M.; Offenberg, J. H.; Kleindienst, T. E.; Edney, E. O.; Sheesley, R. J.; Schauer, J. J. Primary and secondary contributions to ambient PM in the midwestern United States. *Environ. Sci. Technol.* **2008**, *42* (9), 3303−3309.
(25) Kundu, S.; Quraishi, T. A.; Yu, G.; Suarez, C.; Keutsch, F. N.; Stone, E. A. Evidence and quantitation of aromatic organosulfates in ambient aerosols in Lahore, Pakistan. *Atmos. Chem. Phys.* **2013**, *13* (9), 4865−4875.
(26) Roach, P. J.; Laskin, J.; Laskin, A. Nanospray desorption electrospray ionization: An ambient method for liquid-extraction surface sampling in mass spectrometry. *Analyst* **2010**, *135* (9), 2233−2236.
(27) Roach, P. J.; Laskin, J.; Laskin, A. Molecular characterization of organic aerosols using nanospray-desorption/electrospray ionization-mass spectrometry. *Anal. Chem.* **2010**, *82* (19), 7979−7986.
(28) O'Brien, R. E.; Laskin, A.; Laskin, J.; Liu, S.; Weber, R.; Russell, L. M.; Goldstein, A. H. Molecular characterization of organic aerosol using nanospray desorption/electrospray ionization mass spectrometry: CalNex 2010 field study. *Atmos. Environ.* **2013**, *68*, 265−272.
(29) O'Brien, R. E.; Nguyen, T. B.; Laskin, A.; Laskin, J.; Hayes, P. L.; Liu, S.; Jimenez, J. L.; Russell, L. M.; Nizkorodov, S. A.; Goldstein, A. H. Probing molecular associations of field-collected and laboratory-generated SOA with nano-DESI high-resolution mass spectrometry. *J. Geophys. Res.* **2013**, *118* (2), 1042−1051.
(30) Laskin, J.; Laskin, A.; Roach, P. J.; Slysz, G. W.; Anderson, G. A.; Nizkorodov, S. A.; Bones, D. L.; Nguyen, L. Q. High-resolution desorption electrospray ionization mass spectrometry for chemical characterization of organic aerosols. *Anal. Chem.* **2010**, *82* (5), 2048−2058.
(31) Eckert, P. A.; Roach, P. J.; Laskin, A.; Laskin, J. Chemical characterization of crude petroleum using nanospray desorption electrospray ionization coupled with high-resolution mass spectrometry. *Anal. Chem.* **2012**, *84* (3), 1517−1525.
(32) Hayes, P. L.; Ortega, A. M.; Cubison, M. J.; Froyd, K. D.; Zhao, Y.; Cliff, S. S.; Hu, W. W.; Toohey, D. W.; Flynn, J. H.; Lefer, B. L.; Grossberg, N.; Alvarez, S.; Rappenglueck, B.; Taylor, J. W.; Allan, J. D.; Holloway, J. S.; Gilman, J. B.; Kuster, W. C.; De Gouw, J. A.; Massoli, P.; Zhang, X.; Liu, J.; Weber, R. J.; Corrigan, A. L.; Russell, L. M.; Isaacman, G.; Worton, D. R.; Kreisberg, N. M.; Goldstein, A. H.; Thalman, R.; Waxman, E. M.; Volkamer, R.; Lin, Y. H.; Surratt, J. D.; Kleindienst, T. E.; Offenberg, J. H.; Dusanter, S.; Griffith, S.; Stevens, P. S.; Brioude, J.; Angevine, W. M.; Jimenez, J. L. Organic aerosol composition and sources in Pasadena, California during the 2010 CalNex campaign. *J. Geophys. Res.* **2013**, *118* (16), 9233−9257.
(33) Ryerson, T. B.; Andrews, A. E.; Angevine, W. M.; Bates, T. S.; Brock, C. A.; Cairns, B.; Cohen, R. C.; Cooper, O. R.; de Gouw, J. A.; Fehsenfeld, F. C.; Ferrare, R. A.; Fischer, M. L.; Flagan, R. C.; Goldstein, A. H.; Hair, J. W.; Hardesty, R. M.; Hostetler, C. A.; Jimenez, J. L.; Langford, A. O.; McCauley, E.; McKeen, S. A.; Molina, L. T.; Nenes, A.; Oltmans, S. J.; Parrish, D. D.; Pederson, J. R.; Pierce, R. B.; Prather, K.; Quinn, P. K.; Seinfeld, J. H.; Senff, C. J.; Sorooshian, A.; Stutz, J.; Surratt, J. D.; Trainer, M.; Volkamer, R.; Williams, E. J.; Wofsy, S. C. The 2010 California research at the nexus of air quality and climate change (CalNex) field study. *J. Geophys. Res.* **2013**, *118* (11), 5830−5866.
(34) Kim, S.; Kramer, R. W.; Hatcher, P. G. Graphical method for analysis of ultrahigh-resolution broadband mass spectra of natural organic matter, the van Krevelen diagram. *Anal. Chem.* **2003**, *75* (20), 5336−5344.
(35) Paulot, F.; Crounse, J. D.; Kjaergaard, H. G.; Kroll, J. H.; Seinfeld, J. H.; Wennberg, P. O. Isoprene photooxidation: New insights into the production of acids and organic nitrates. *Atmos. Chem. Phys.* **2009**, *9* (4), 1479−1501.
(36) Hu, K. S.; Darer, A. I.; Elrod, M. J. Thermodynamics and kinetics of the hydrolysis of atmospherically relevant organonitrates and organosulfates. *Atmos. Chem. Phys.* **2011**, *11* (16), 8307−8320.
(37) Gomez-Gonzalez, Y.; Surratt, J. D.; Cuyckens, F.; Szmigielski, R.; Vermeylen, R.; Jaoui, M.; Lewandowski, M.; Offenberg, J. H.; Kleindienst, T. E.; Edney, E. O.; Blockhuys, F.; Van Alsenoy, C.; Maenhaut, W.; Claeys, M. Characterization of organosulfates from the photooxidation of isoprene and unsaturated fatty acids in ambient aerosol using liquid chromatography/(−) electrospray ionization mass spectrometry. *J. Mass Spectrom.* **2008**, *43* (3), 371−382.
(38) Nguyen, T. B.; Lee, P. B.; Updyke, K. M.; Bones, D. L.; Laskin, J.; Laskin, A.; Nizkorodov, S. A. Formation of nitrogen- and sulfur-containing light-absorbing compounds accelerated by evaporation of water from secondary organic aerosols. *J. Geophys. Res.* **2012**, *117*, DOI: 10.1029/2011JD016944.
(39) Wang, X. F.; Zhang, Y. P.; Chen, H.; Yang, X.; Chen, J. M.; Geng, F. H. Particulate nitrate formation in a highly polluted urban area: A case study by single-particle mass spectrometry in Shanghai. *Environ. Sci. Technol.* **2009**, *43* (9), 3061−3066.
(40) He, K.; Zhao, Q.; Ma, Y.; Duan, F.; Yang, F.; Shi, Z.; Chen, G. Spatial and seasonal variability of PM2.5 acidity at two Chinese megacities: Insights into the formation of secondary inorganic aerosols. *Atmos. Chem. Phys.* **2012**, *12* (3), 1377−1395.
(41) Huang, Y.; Li, L.; Li, J.; Wang, X.; Chen, H.; Chen, J.; Yang, X.; Gross, D. S.; Wang, H.; Qiao, L.; Chen, C. A case study of the highly time-resolved evolution of aerosol chemical and optical properties in urban Shanghai, China. *Atmos. Chem. Phys.* **2013**, *13* (8), 3931−3944.
(42) Gao, S.; Ng, N. L.; Keywood, M.; Varutbangkul, V.; Bahreini, R.; Nenes, A.; He, J. W.; Yoo, K. Y.; Beauchamp, J. L.; Hodyss, R. P.; Flagan, R. C.; Seinfeld, J. H. Particle phase acidity and oligomer formation in secondary organic aerosol. *Environ. Sci. Technol.* **2004**, *38* (24), 6582−6589.
(43) Hall, W. A.; Johnston, M. V. Oligomer formation pathways in secondary organic aerosol from MS and MS/MS measurements with high mass accuracy and resolving power. *J. Am. Soc. Mass Spectrom.* **2012**, *23* (6), 1097−1108.
(44) Tobias, H. J.; Beving, D. E.; Ziemann, P. J.; Sakurai, H.; Zuk, M.; McMurry, P. H.; Zarling, D.; Waytulonis, R.; Kittelson, D. B. Chemical analysis of diesel engine nanoparticles using a nano-DMA/thermal desorption particle beam mass spectrometer. *Environ. Sci. Technol.* **2001**, *35* (11), 2233−2243.
(45) Sakurai, H.; Tobias, H. J.; Park, K.; Zarling, D.; Docherty, K. S.; Kittelson, D. B.; McMurry, P. H.; Ziemann, P. J. On-line measurements of diesel nanoparticle composition and volatility. *Atmos. Environ.* **2003**, *37* (9−10), 1199−1210.
(46) Schauer, J. J.; Kleeman, M. J.; Cass, G. R.; Simoneit, B. Measurement of emissions from air pollution sources. 2. C-1 through

C-30 organic compounds from medium duty diesel trucks. *Environ. Sci. Technol.* **1999**, *33* (10), 1578−1587.
(47) Schauer, J. J.; Kleeman, M. J.; Cass, G. R.; Simoneit, B. Measurement of emissions from air pollution sources. 5. C-1−C-32 organic compounds from gasoline-powered motor vehicles. *Environ. Sci. Technol.* **2002**, *36* (6), 1169−1180.
(48) Lim, Y. B.; Ziemann, P. J. Effects of molecular structure on aerosol yields from OH radical-initiated reactions of linear, branched, and cyclic alkanes in the presence of NOx. *Environ. Sci. Technol.* **2009**, *43* (7), 2328−2334.
(49) Yee, L. D.; Craven, J. S.; Loza, C. L.; Schilling, K. A.; Ng, N. L.; Canagaratna, M. R.; Ziemann, P. J.; Flagan, R. C.; Seinfeld, J. H. Effect of chemical structure on secondary organic aerosol formation from C-12 alkanes. *Atmos. Chem. Phys.* **2013**, *13* (21), 11121−11140.
(50) Jobson, B. T.; Berkowitz, C. M.; Kuster, W. C.; Goldan, P. D.; Williams, E. J.; Fesenfeld, F. C.; Apel, E. C.; Karl, T.; Lonneman, W. A.; Riemer, D. Hydrocarbon source signatures in Houston, Texas: Influence of the petrochemical industry. *J. Geophys. Res.* **2004**, *109*, DOI: 10.1029/2004JD004887.
(51) Wang, H. L.; Chen, C. H.; Wang, Q.; Huang, C.; Su, L. Y.; Huang, H. Y.; Lou, S. R.; Zhou, M.; Li, L.; Qiao, L. P.; Wang, Y. H. Chemical loss of volatile organic compounds and its impact on the source analysis through a two-year continuous measurement. *Atmos. Environ.* **2013**, *80*, 488−498.
(52) Simoneit, B. Biomass burning—A review of organic tracers for smoke from incomplete combustion. *Appl. Geochem.* **2002**, *17* (3), 129−162.
(53) He, L. Y.; Lin, Y.; Huang, X. F.; Guo, S.; Xue, L.; Su, Q.; Hu, M.; Luan, S. J.; Zhang, Y. H. Characterization of high-resolution aerosol mass spectra of primary organic aerosol emissions from Chinese cooking and biomass burning. *Atmos. Chem. Phys.* **2010**, *10* (23), 11535−11543.
(54) Nolte, C. G.; Schauer, J. J.; Cass, G. R.; Simoneit, B. Highly polar organic compounds present in meat smoke. *Environ. Sci. Technol.* **1999**, *33* (19), 3313−3316.
(55) Cai, C.; Geng, F.; Tie, X.; Yu, Q.; Peng, L.; Zhou, G. Characteristics of ambient volatile organic compounds (VOCs) measured in Shanghai, China. *Sensors* **2010**, *10* (8), 7843−7862.
(56) Cai, C.; Geng, F.; Tie, X.; Yu, Q.; An, J. Characteristics and source apportionment of VOCs measured in Shanghai, China. *Atmos. Environ.* **2010**, *44* (38), 5005−5014.
(57) Decesari, S.; Finessi, E.; Rinaldi, M.; Paglione, M.; Fuzzi, S.; Stephanou, E. G.; Tziaras, T.; Spyros, A.; Ceburnis, D.; O'Dowd, C.; Dall'Osto, M.; Harrison, R. M.; Allan, J.; Coe, H.; Facchini, M. C. Primary and secondary marine organic aerosols over the North Atlantic Ocean during the MAP experiment. *J. Geophys. Res.* **2011**, *116*, DOI: 10.1029/2011JD016204.
(58) Becagli, S.; Ghedini, C.; Peeters, S.; Rottiers, A.; Traversi, R.; Udisti, R.; Chiari, M.; Jalba, A.; Despiau, S.; Dayan, U.; Temara, A. MBAS (methylene blue active substances) and LAS (linear alkylbenzene sulphonates) in Mediterranean coastal aerosols: Sources and transport processes. *Atmos. Environ.* **2011**, *45* (37), 6788−6801.
(59) Facchini, M. C.; Mircea, M.; Fuzzi, S.; Charlson, R. J. Cloud albedo enhancement by surface-active organic solutes in growing droplets. *Nature* **1999**, *401* (6750), 257−259.